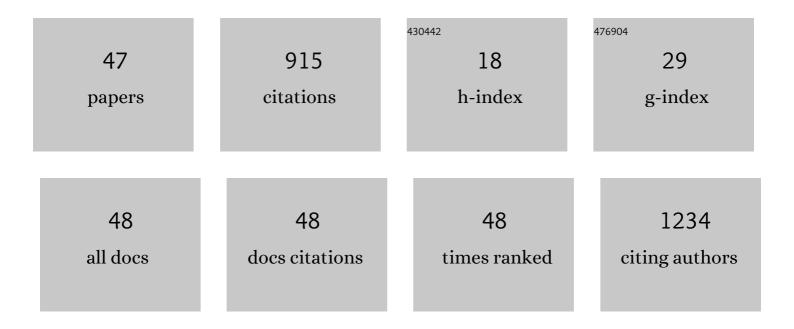
Giuseppe Ferrauto

List of Publications by Year in descending order

Source: https://exaly.com/author-pdf/9544873/publications.pdf Version: 2024-02-01



#	Article	IF	CITATIONS
1	In vivo maps of extracellular pH in murine melanoma by CEST–MRI. Magnetic Resonance in Medicine, 2014, 71, 326-332.	1.9	98
2	In vivo MRI visualization of different cell populations labeled with PARACEST agents. Magnetic Resonance in Medicine, 2013, 69, 1703-1711.	1.9	58
3	Lanthanide-Loaded Erythrocytes As Highly Sensitive Chemical Exchange Saturation Transfer MRI Contrast Agents. Journal of the American Chemical Society, 2014, 136, 638-641.	6.6	47
4	The Issue of Gadolinium Retained in Tissues. Investigative Radiology, 2018, 53, 167-172.	3.5	44
5	Eight-Coordinate, Stable Fe(II) Complex as a Dual ¹⁹ F and CEST Contrast Agent for Ratiometric pH Imaging. Inorganic Chemistry, 2017, 56, 12206-12213.	1.9	41
6	LipoCEST and cellCEST imaging agents: opportunities and challenges. Wiley Interdisciplinary Reviews: Nanomedicine and Nanobiotechnology, 2016, 8, 602-618.	3.3	40
7	Gd loading by hypotonic swelling: an efficient and safe route for cellular labeling. Contrast Media and Molecular Imaging, 2013, 8, 475-486.	0.4	37
8	An MRI Method To Map Tumor Hypoxia Using Red Blood Cells Loaded with a pO ₂ -Responsive Gd-Agent. ACS Nano, 2015, 9, 8239-8248.	7.3	36
9	Large photoacoustic effect enhancement for ICG confined inside MCM-41 mesoporous silica nanoparticles. Nanoscale, 2017, 9, 99-103.	2.8	34
10	Re-evaluation of the water exchange lifetime value across red blood cell membrane. Biochimica Et Biophysica Acta - Biomembranes, 2016, 1858, 627-631.	1.4	33
11	Advanced cardiac chemical exchange saturation transfer (cardioCEST) MRI for <i>in vivo</i> cell tracking and metabolic imaging. NMR in Biomedicine, 2016, 29, 74-83.	1.6	32
12	Gd-loaded-RBCs for the assessment of tumor vascular volume byÂcontrast-enhanced-MRI. Biomaterials, 2015, 58, 82-92.	5.7	29
13	Simultaneous MR imaging for tissue engineering in a rat model of stroke. Scientific Reports, 2015, 5, 14597.	1.6	26
14	CESTâ€MRI for glioma pH quantification in mouse model: Validation by immunohistochemistry. NMR in Biomedicine, 2018, 31, e4005.	1.6	26
15	Frequency-Encoded MRI-CEST Agents Based on Paramagnetic Liposomes/RBC Aggregates. Nano Letters, 2014, 14, 6857-6862.	4.5	24
16	Gd accumulation in tissues of healthy mice upon repeated administrations of Gadodiamide and Gadoteridol. Journal of Trace Elements in Medicine and Biology, 2018, 48, 239-245.	1.5	23
17	Activation of the <scp>MET</scp> receptor attenuates doxorubicinâ€induced cardiotoxicity in vivo and in vitro. British Journal of Pharmacology, 2020, 177, 3107-3122.	2.7	20
18	MRI nanoprobes based on chemical exchange saturation transfer: Ln ^{III} chelates anchored on the surface of mesoporous silica nanoparticles. Nanoscale, 2014, 6, 9604-9607.	2.8	19

GIUSEPPE FERRAUTO

#	Article	IF	CITATIONS
19	Enzymeâ€Responsive LipoCEST Agents: Assessment of MMPâ€2 Activity by Measuring the Intraâ€liposomal Water ¹ Hâ€NMR Shift. Angewandte Chemie - International Edition, 2017, 56, 12170-12173.	7.2	19
20	Complete on/off responsive ParaCEST MRI contrast agents for copper and zinc. Dalton Transactions, 2018, 47, 11346-11357.	1.6	19
21	Insights on the relaxation of liposomes encapsulating paramagnetic Lnâ€based complexes. Magnetic Resonance in Medicine, 2015, 74, 468-473.	1.9	15
22	CESTâ€MRI studies of cells loaded with lanthanide shift reagents. Magnetic Resonance in Medicine, 2018, 80, 1626-1637.	1.9	15
23	Optimizing the Relaxivity of MRI Probes at High Magnetic Field Strengths With Binuclear GdIII Complexes. Frontiers in Chemistry, 2018, 6, 158.	1.8	14
24	Relaxometric studies of erythrocyte suspensions infected by <i>Plasmodium falciparum</i> : a tool for staging infection and testing antiâ€malarial drugs. Magnetic Resonance in Medicine, 2020, 84, 3366-3378.	1.9	13
25	Acid-catalyzed proton exchange as a novel approach for relaxivity enhancement in Gd-HPDO3A-like complexes. Chemical Science, 2020, 11, 7829-7835.	3.7	13
26	Photoacoustic ratiometric assessment of mitoxantrone release from theranostic ICG-conjugated mesoporous silica nanoparticles. Nanoscale, 2019, 11, 18031-18036.	2.8	12
27	Toll-like receptor 2 promotes breast cancer progression and resistance to chemotherapy. Oncolmmunology, 2022, 11, .	2.1	12
28	Sensitive MRI detection of internalized <i>T</i> ₁ contrast agents using magnetization transfer contrast. NMR in Biomedicine, 2015, 28, 1663-1670.	1.6	11
29	Modulation of the Prototropic Exchange Rate in pHâ€Responsive Ybâ€HPDO3A Derivatives as ParaCEST Agents. ChemistrySelect, 2018, 3, 6035-6041.	0.7	11
30	Mn(<scp>ii</scp>)-Conjugated silica nanoparticles as potential MRI probes. Journal of Materials Chemistry B, 2021, 9, 8994-9004.	2.9	9
31	Use of FCC-NMRD relaxometry for early detection and characterization of ex-vivo murine breast cancer. Scientific Reports, 2019, 9, 4624.	1.6	8
32	Modifying LnHPDO3A Chelates for Improved <i>T</i> ₁ and CEST MRI Applications. Chemistry - A European Journal, 2019, 25, 4184-4193.	1.7	8
33	Detection of U-87 Tumor Cells by RGD-Functionalized/Gd-Containing Giant Unilamellar Vesicles in Magnetization Transfer Contrast Magnetic Resonance Images. Investigative Radiology, 2021, 56, 301-312.	3.5	8
34	Enzymeâ€Responsive LipoCEST Agents: Assessment of MMPâ€2 Activity by Measuring the Intraâ€liposomal Water ¹ Hâ€NMR Shift. Angewandte Chemie, 2017, 129, 12338-12341.	1.6	7
35	Generation of multiparametric MRI maps by using Gd-labelled- RBCs reveals phenotypes and stages of murine prostate cancer. Scientific Reports, 2018, 8, 10567.	1.6	7
36	A Simple and Fast Assay Based on Carboxyfluorescein-Loaded Liposome for Quantitative DNA Detection. ACS Omega, 2020, 5, 1764-1772.	1.6	7

GIUSEPPE FERRAUTO

#	Article	IF	CITATIONS
37	Supramolecular adducts between macrocyclic Gd(<scp>iii</scp>) complexes and polyaromatic systems: a route to enhance the relaxivity through the formation of hydrophobic interactions. Chemical Science, 2021, 12, 1368-1377.	3.7	7
38	Chapter 3. Chemical Exchange Saturation Transfer (CEST) Contrast Agents. New Developments in NMR, 2017, , 243-317.	0.1	7
39	Development and characterization of lanthanide-HPDO3A-C16-based micelles as CEST-MRI contrast agents. Dalton Transactions, 2019, 48, 5343-5351.	1.6	6
40	Multilamellar LipoCEST Agents Obtained from Osmotic Shrinkage of Paramagnetically Loaded Giant Unilamellar Vescicles (GUVs). Angewandte Chemie - International Edition, 2020, 59, 2279-2283.	7.2	5
41	The interaction between iodinated Xâ€ray contrast agents and macrocyclic <scp>GBCAs</scp> provides a signal enhancement in <scp>T₁â€weighted MR</scp> images: Insights into the renal excretion pathways of <scp>Gdâ€HPDO3A</scp> and iodixanol in healthy mice. Magnetic Resonance in Medicine. 2022. 88. 357-364.	1.9	4
42	Water Diffusion Modulates the CEST Effect on Tb(III)-Mesoporous Silica Probes. Magnetochemistry, 2020, 6, 38.	1.0	3
43	Compartmentalized agents: A powerful strategy for enhancing the detection sensitivity of chemical exchange saturation transfer contrast. NMR in Biomedicine, 2023, 36, .	1.6	3
44	Multilamellar LipoCEST Agents Obtained from Osmotic Shrinkage of Paramagnetically Loaded Giant Unilamellar Vescicles (GUVs). Angewandte Chemie, 2020, 132, 2299-2303.	1.6	2
45	LipHosomes: Reporters for Ligand/Antiâ€Ligand Assays Based On pH Readout. Analysis & Sensing, 2021, 1, 48-53.	1.1	1
46	Effects of Cations on HPTS Fluorescence and Quantification of Free Gadolinium Ions in Solution; Assessment of Intracellular Release of Gd3+ from Gd-Based MRI Contrast Agents. Molecules, 2022, 27, 2490.	1.7	1
47	Studies of the hydrophobic interaction between a pyrene-containing dye and a tetra-aza macrocyclic gadolinium complex. Inorganic Chemistry Frontiers, 2022, 9, 3494-3504.	3.0	1